

CFD Study of the Fire Response of Vessels Containing Liquefied Gases

Giordano Scarponi^{a,*}, Gabriele Landucci^{b,c}, Albrecht Michael Birk^d, Valerio Cozzani^a

^a LISES - Department of Civil, Chemical, Environmental and Material Engineering, Alma Mater Studiorum – University of Bologna, via Terracini 28, 40131, Bologna (Italy)

^b Department of Civil and Industrial Engineering, University of Pisa, Largo Lucio Lazzarino 2, 56126, Pisa (Italy)

^c Institute of Security and Global Affairs, Faculty of Governance and Global Affairs, Leiden University, Wijnhaven, Turfmarkt 99, 2511 DP, Den Haag (the Netherlands)

^d Dept. of Mechanical and Materials Engineering, McLaughlin Hall, Queen's University, Kingston, ON, Canada K7L 3N6
valerio.cozzani@unibo.it

Accidental fires represent a serious threat for vessels devoted to the transportation and storage of liquefied gases, such as propane and butane. The present work focuses the impact of full engulfing hydrocarbon pool fires on propane and butane storage tanks. The analysis was carried out using a computational fluid dynamics (CFD) model, previously validated against experimental data. Results are presented in terms of pressurization rates, and temperature distributions showing the difference in the response to fire between propane and butane tanks. The effect of the filling degree is also pointed out. The outcomes of this work provide useful results to evaluate the possible failure conditions, thus supporting the emergency response to accidental fires in the proximity of storage tanks or transport units.

1. Introduction

Accidental fires represent a serious threat for vessels devoted to the transportation or storage of liquefied gases, such as propane and butane (D'Aulisa et al. 2014). In fact, the heat load generated by the fire can induce the thermal failure of the vessels, leading to extremely dangerous events like boiling liquid expanding vapor explosion (Landucci et al. 2013), fireball (Landucci et al., 2015) and missiles projection (Tugnoli et al., 2014). Therefore, being able to predict how fast the pressure will rise under a given fire load and to quantify the energy content of the vessel at the moment of failure would represent a valuable advantage for tanks designer and for those involved in the emergency response and management. Traditional lumped models suffer several limitations and are not able to predict pressurization and temperature distributions with confidence (Landucci et al. 2016). With the aim of characterizing and predicting the response of pressurized tanks exposed to fire, Scarponi et al. (2018a) proposed a two-dimensional (2D) model, based on computational fluid dynamics (CFD). This was validated against data from an extended set of fire test simulating full engulfing pool fire scenarios affecting liquefied petroleum gas (LPG) tanks. Simulations of a fire test considering a distance heat source were also carried out (Scarponi et al. 2018b). In all the cases, the model predictions showed a good agreement with the experimental measurements in terms of pressure and temperatures, proving the robustness of the modelling setup. Despite the variety of simulated scenarios (different tank size, filling degree, fire conditions), the analysis was always limited to tanks devoted to store LPG assumed as pure propane, hence the effect of liquid composition and heavier components, such as butane, was not taken into account in modelling the vessel response to fire. In the present work, the above mentioned CFD modelling approach was extended to pressure tanks containing liquid n-butane, thus addressing the effect of LPG composition on the pressure build-up, pointing out differences and similarities in the thermo-fluid dynamic behaviour of propane and butane, and highlighting crucial aspects from the safety point of view. The effect of different filling degree was also taken into account, in order to investigate complicating phenomena, such as thermal stratification induced by the tank heat-up.

Paper Received: 1 March 2019; Revised: 9 April 2019; Accepted: 16 June 2019

Please cite this article as: Scarponi G., Landucci G., Birk A., Cozzani V., 2019, CFD Study of the Fire Response of Vessels Containing Liquefied Gases, Chemical Engineering Transactions, 77, 373-378 DOI:10.3303/CET1977063

2. Overview of the modelling approach

2.1 Model equations and solution methods

The CFD model was based on the solution of the conservative equation for mass, momentum, energy (solved also in the solid domain) and turbulent quantities reported in Table 1. All the simulations were carried out using the software ANSYS® Fluent® 18.2.0.

Table 1: CFD model equations

Property	Equations	
Volume fraction of the secondary phase (liquid)	$\frac{\partial}{\partial t}(\alpha_L \rho_L) + \nabla \cdot (\alpha_L \rho_L \vec{u}_L) = \dot{m}_{V \rightarrow L} - \dot{m}_{L \rightarrow V}$	(1)
	ρ_L : liquid density; t : time; α_L : liquid volume fraction; \vec{u}_L : Reynolds averaged velocity;	
	$\text{if } T > T_{sat} \quad m_{L \rightarrow V} = C_E \alpha_L \rho_L \left(\frac{T - T_{sat}}{T_{sat}} \right), m_{V \rightarrow L} = 0$	(2)
Mass transfer equations	$\text{if } T > T_{sat} \quad m_{L \rightarrow V} = 0, m_{V \rightarrow L} = C_C \alpha_V \rho_V \left(\frac{T_{sat} - T}{T_{sat}} \right)$	(3)
	T : temperature; T_{sat} : saturation temperature; C_E and C_C : coefficients (both set to the default value of 0.1 s^{-1})	
Volume fraction of the primary phase (vapor)	$\alpha_V = 1 - \alpha_L$	(4)
	α_V : vapor volume fraction	
	$\varphi = \varphi_V \alpha_V + \varphi_L \alpha_L$	(5)
Two-phase averaged quantity	Two-phase volume fraction averaged property φ function of liquid and vapor properties (φ_L and φ_V , respectively) where φ can be density ρ , viscosity μ , turbulent viscosity μ_T , thermal conductivity k .	
Momentum	$\frac{\partial}{\partial t}(\rho \vec{u}) + \nabla \cdot (\rho \vec{u} \vec{u}) = -\nabla p + \nabla \cdot \left[\mu (\nabla \vec{u} + \nabla \vec{u}^T) - \frac{2}{3} \mu \nabla \cdot \vec{u} I \right] + \rho \vec{g} + \vec{F} - \nabla \cdot \tau'$	(6)
	ρ : two-phase volume fraction averaged density; p : Reynolds averaged pressure; μ : two-phase averaged viscosity; g : gravity acceleration; I : identity tensor.	
Reynolds stress tensor (introducing the Boussinesq approximation)	$\tau' = \mu_T [(\nabla \vec{u} + \nabla \vec{u}^T)] - \frac{2}{3} (\rho K + \mu_T \nabla \cdot \vec{u} I)$	(7)
	μ_T : two-phase averaged turbulent viscosity; K : turbulent kinetic energy	
Turbulent viscosity	$\mu_T = \frac{\rho K}{\omega} L$	(8)
	ω : Turbulent specific dissipation rate; the definition of L can be found in [48]	
Turbulent kinetic energy	$\frac{\partial}{\partial t}(\rho K) + \nabla \cdot (\rho K \vec{u}) = \nabla \cdot (\Gamma_K \nabla K) + G_K - Y_K$	(9)
	Γ_K : turbulent Prandtl number for K ; G_K : generation of K due to mean velocity gradients; Y_K : dissipation of K due to turbulence. The definitions of Γ_K , G_K and Y_K can be found in [48]	
Turbulent specific dissipation rate	$\frac{\partial}{\partial t}(\rho \omega) + \nabla \cdot (\rho \omega \vec{u}) = \nabla \cdot (\Gamma_\omega \nabla \omega) + G_\omega - Y_\omega$	(10)
	Γ_ω : turbulent Prandtl number for ω ; G_ω : generation of ω ; Y_ω : dissipation of ω . The definitions of Γ_ω , G_ω and Y_ω can be found in ANSYS inc (2012).	
Energy (fluid domain)	$\frac{\partial}{\partial t}(\rho E) + \nabla \cdot (\vec{u}(\rho E + p)) = -\nabla p + \nabla \cdot [k_{eff} \nabla T] + \Delta H_{vap}(\dot{m}_{V \rightarrow L} - \dot{m}_{L \rightarrow V})$	(11)
	E : two-phase Reynolds averaged specific energy; k_{eff} : effective thermal conductivity; λ : heat of vaporization;	
Energy (solid domain)	$\frac{\partial}{\partial t}(\rho_s C_p T_s) = \nabla \cdot (k_s \nabla T_s)$	(12)
	T_s : temperature in the solid; k_s : steel thermal conductivity; ρ_s steel density; C_p steel heat capacity	
Effective thermal conductivity	$k_{eff} = k + \frac{c_p \mu_T}{Pr_T}$	(13)
	k = two-phase volume fraction averaged thermal conductivity c_p : two-phase volume fraction averaged heat capacity, Pr_T : turbulent Prandtl number = 0.85	

Fluid properties of the substances considered (pure propane and pure n-butane, in the following indicated as “butane”) are expressed as a function of temperature adopting the thermodynamic dataset reported in Liley et al. (1999). The Soave-Redlich-Kwong state equation was considered to be valid for the vapor phase. The thermal properties of carbon steel for the tank wall were taken from (CEN, 1998). All the simulations were run until the pressure reached the pressure relief valve (PRV) set point, with a time step of 5 ms, considering a first order implicit scheme for the transient formulation. At each time step, the solution was considered converged when one of the following criteria was satisfied:

- The sum of the scaled residuals was below 10^{-3}
- For a given time step, the ratio between the residuals and the residuals at the beginning of the time step was below 0.05

Pressure and velocity coupling was obtained by means of the SIMPLEC (Semi-Implicit Method for Pressure Linked Equations-Consistent) algorithm. For what concerns the spatial discretization, a second order upwind scheme was chosen for density, momentum, energy and turbulent quantities (k and ω), whereas the PRESTO! and the Geo-Reconstruction schemes were used for the pressure and the volume fraction respectively (ANSYS inc, 2012).

2.2 Case study and fire scenario definition

In order to analyse the differences in the behaviour of propane and butane storage tank under fire exposure, a set of case studies was defined (see Table 2). The same tank was considered for both substances, with a diameter of 1 m and a wall thickness of 6 mm. The filling degree was varied simulating considering a situation in which the liquid occupies the 20%, the 50% and the 80% of the total volume.

Table 2: List of case studies considered in the present work.

Case number	Case ID	Substance	Filling degree
1	B_20	Butane	20 %
2	B_50	Butane	50 %
3	B_80	Butane	80 %
4	P_20	Propane	20 %
5	P_50	Propane	50 %
6	P_80	Propane	80 %

The scenario taken into consideration is full engulfing pool fire with a black body temperature of 871°C, according to the guidelines proposed by Anderson et al. (1974), Birk et al. (2016) and Scarponi et al. (2017). In order to be conservative, the emissivity of the tank wall was set to 1. At the beginning of the simulations, the tank lading was assumed to be motionless and at the saturation pressure at 20°C. Turbulent kinetic energy and specific dissipation rate were initialized at $10^{-9} \text{ m}^2/\text{s}^2$ and 10^{-3} s^{-1} respectively. The no slip condition was set at the inner wall, whereas symmetry was considered at the vertical tank centerline.

2.3 Computational domain and grid definition

The computational domain consists of a 2D vertical (and perpendicular to the axial direction) section of cylindrical tank positioned horizontally. The grid is unstructured and is formed by a combination of quadrilateral and triangular elements. The maximum cell size was 30 mm with a global growth rate of 1.1. The inner and the outer wall were divided in the same number of segments, so that each segment on the outer wall was approximately 2 mm-long. In order to ensure a good resolution in the near wall region, 25 inflation layers were built starting from the inner wall of the tank with a growth rate of 1.2. The first layer thickness was set to 0.2 mm.

3. Results and discussion

Fire exposure determines an increase in the internal pressure of the tank due to the heat-up of the lading. Figure 2 shows the pressurization curves obtained for the cases listed in Table 2. Quite clearly, due to the higher volatility of the stored substance, the cases in which propane tanks are simulated exhibit a faster pressurization than those in which butane is considered. In fact, in cases P_20, P_50 and P_80, the PRV opening set point is reached after a fire exposure period of 120s, 140s and 115s, respectively. This time is more than doubled for the cases involving butane (260s, 275s and 340s for cases B_20, B_50, and B_80 respectively). Figure 1 also shows the effect of the filling degree. For both substances, the lowest pressurization curve was obtained in the 50% filling cases (Cases 2 and 5, respectively for butane and propane). This situation changes considering the other two filling conditions. As far as cases involving propane are concerned, the PRV opening pressure is reached earlier when the tank is almost full of liquid (80% filling

degree). On the other contrary, when tanks storing butane are considered, the PRV set point is reached first for the lowest filling degree case (B_20).

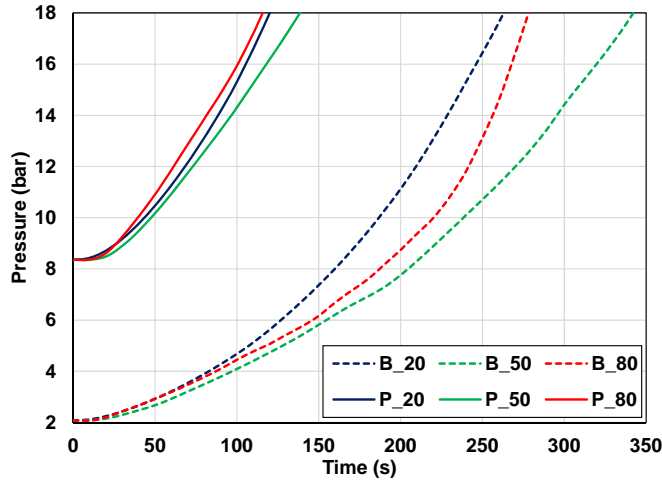


Figure 2: Pressurization curves obtained for the three case studies listed in Table 2, to which the Reader is referred for cases identification. Solid lines represent the cases in which propane is simulated, while dashed lines the ones with butane.

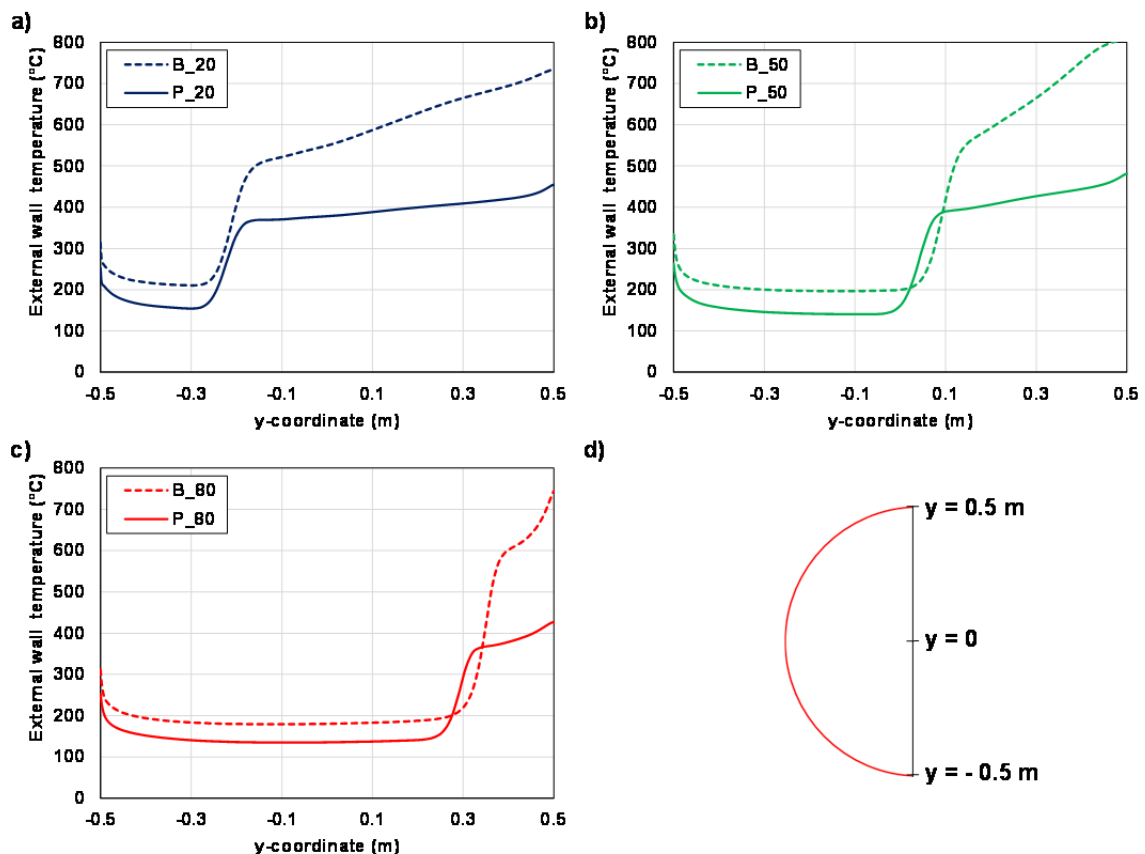


Figure 3: Outer wall temperature profiles at PRV opening function of the y-coordinate (as defined in panel d) for simulations at different filling degrees: a) 20%; b) 50%; c) 80%. Solid lines represent the cases in which propane is simulated, while dashed lines the ones with butane. For cases identification refer to Table 2.

Besides pressurization, one of the key factors affecting the vessel integrity during fire exposure is the wall temperature. In fact, carbon steel suffers severe weakening at temperatures above 400°C (Cotgreave, 1992). Furthermore, creep becomes important beyond this temperature and the tank wall begins suffering thinning phenomena that can rapidly result in the formation of a small hole in the vapor region, which can then propagate and lead to a total loss of containment (Manu et al., 2009).

Figure 3 compares the temperature distributions along the tank wall obtained for the case studies listed in Table 2 at the instant of time when the pressure reaches the PRV set point (i.e., the end of each simulation). In all the cases, it is well visible the cooling effect of the liquid on the tank wall. On the other hand, the vapor wetted wall attains higher temperatures. This is more evident for the cases involving butane, for which values between 500°C and 800°C are registered. This is due to the fact that the pressurization of butane tanks is slowed down by the lower substance volatility, resulting in a more prolonged fire exposure before the PRV opening, hence in a high energy accumulation in the tank leading and a marked increment in wall temperature. At such high temperatures, the steel strength is severely compromised (Cotgreave, 1992) and the tank would most probably fail well before the PRV activation. This is a very important aspect to take into account when considering safety measures aimed at reducing the risk of the tank collapse in case of fire exposure. In fact, the PRV (when present and if properly sized) only allows to avoid that the pressure inside the tank reaches the design limits, but it has no relevant effect on the weakening of construction material due to heat exposure, as remarked in previous studies (Landucci et al., 2013).

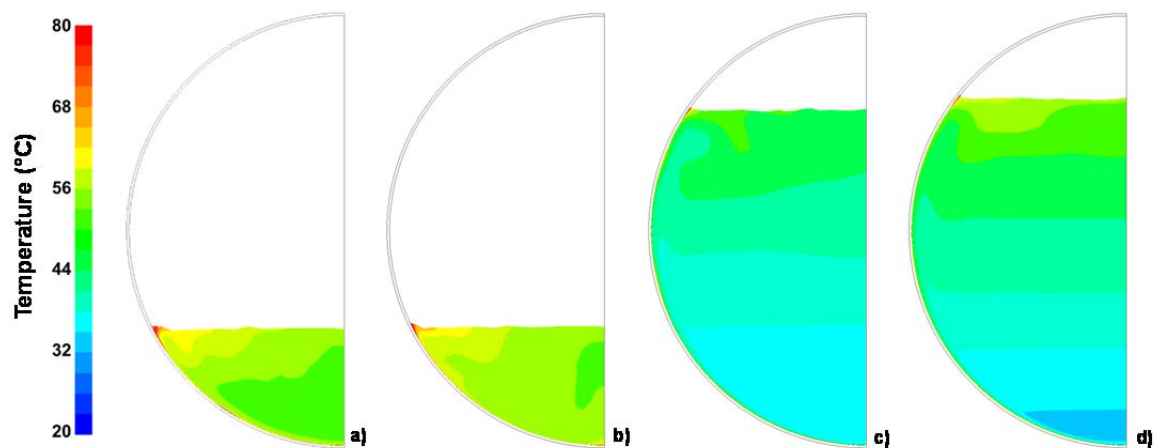


Figure 4: Temperature contour plots in °C calculated for the liquid phase after 120s for the following cases: B_20 (a), P_20 (b), B_80 (c) and P_80 (d). For cases identification refer to Table 2.

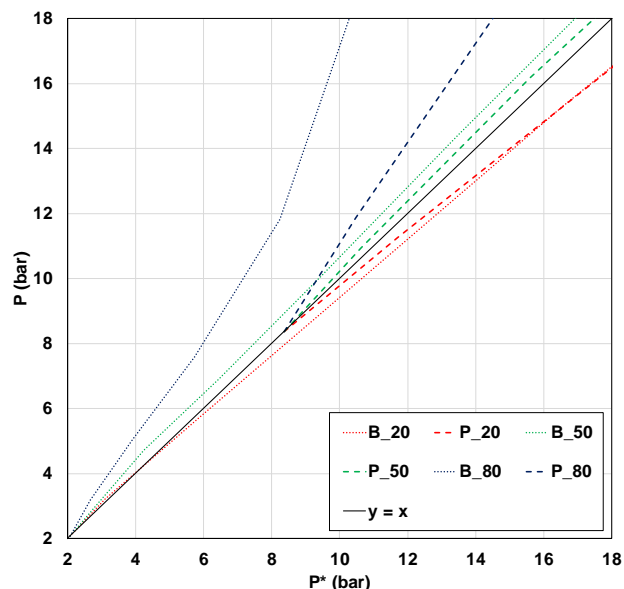


Figure 5: Comparison between the tank pressure, P , and the saturation pressure calculated at the average liquid temperature, P^* . For cases identification refer to Table 2.

Figure 4 compares the temperature contour plots below the liquid surface obtained for both butane and propane cases with the lowest (B_20 and P_20) and the highest (B_80 and P_80) filling degree after 120s of fire exposure. In the low filling level conditions (see Figures 4a and 4b), the temperature is more uniform than

in the high filling level conditions (Figures 4c and 4d), where the thermal stratification is quite evident and may have a relevant influence on the pressurization rate.

In order to investigate this latter phenomenon, Figure 5 shows the comparison between the predicted tank pressure (P) and the saturation pressure (P^*) estimated at the average liquid temperature. Similar qualitative results are obtained for propane and butane. In fact, in the B_80 and P_80 cases, P is much higher than P^* . On the other hand, P and P^* almost coincide in the cases with the intermediate filling degree (B_50 and P_50). Finally, the liquid phase in the B_20 and P_20 appears to be slightly superheated, with P^* exceeding P of almost 2 bar at the end of the simulations.

4. Conclusions

In the present work, a CFD modelling approach was developed to simulate the behaviour of pressurized tanks exposed to fire. In particular, the aim of the work was to investigate differences and similarities in the response to a full engulfing hydrocarbon pool fire between propane and butane storage tanks. The pressurization of propane tanks is much faster due to the higher volatility, and the elapsed time from the fire start and until the first PRV opening is less than a half with respects to cases involving butane. However, the lower pressurization rate observed for butane storage tanks allow the wall temperatures to reach very high values, at which steel mechanical properties are compromised, especially in the vapour phase. This represents a critical issue. In fact, if no safety measure is put in place to cool down the tank in absence of fireproofing, the failure of the tank may probably occur before the PRV intervenes to limit the pressure rise. This kind of outcome can result very useful to improve storage safety and to support the emergency response planning. Another interesting aspect pointed out by the CFD simulations is the role played by thermal stratification in the tank pressurization. Both for propane and butane, this phenomenon is well visible in the cases with the highest filling degree. On the contrary, it appears to be negligible when less the half of the tank volume is occupied by the liquid phase.

References

- Anderson C.E., Townsend W., Zook J., Cowgill G., 1974, The effects of fire engulfment on a rail tank car filled with LPG, US DOT FRA1974.
- ANSYS® FLUENT® 14.5, 2012 Theory Guide, Cecil Township, PA: ANSYS Inc.
- Birk A. M., Otremba F., Borch J., Bradley I., Bisby L., 2016, Fire Testing of Total Containment Pressure Vessels, *Chemical Engineering Transactions*, 48, 277-282.
- CEN - European Committee for Standardization, 1998, EN 10222-1, Steel forgings for pressure purposes. Part 1: General requirements for open die forgings. Brussels, Belgium: European Committee for Standardization.
- Cotgreave T., 1992, Passive fire protection: performance requirements and test methods, OTI Report 92606, prepared by Steel Construction Institute for HSE, London.
- D'Aulisa A., Tugnoli A., Cozzani V., Landucci G., Birk A.M., 2014, CFD modeling of LPG vessels under fire exposure conditions, *AIChE J.* 60, 4292–4305.
- Landucci G., Cozzani V., Birk, M., 2013, Heat Radiation Effects, in Reniers, G. and Cozzani, V. Eds., *Domino Effects in the Process Industries: Modelling, Prevention and Managing*, 70-115
- Landucci G., D'Aulisa A., Tugnoli A., Cozzani V., Birk A. M., 2016, Modeling heat transfer and pressure build-up in LPG vessels exposed to fires, *International Journal of Thermal Sciences*, 104, 228–244.
- Landucci G., Reniers G., Cozzani V., Salzano E., 2015, Vulnerability of industrial facilities to attacks with improvised explosive devices aimed at triggering domino scenarios, *Reliab. Eng. Syst. Saf.*, 143, 53-62.
- Liley P.E., Thomson G.H., Friend D.G., Daubert T.E., Buck E., 1999, Physical and chemical data, Section 2, In *Perry's chemical engineers' handbook* (7th ed.), New York, NY: McGraw Hill.
- Manu C.C., Birk A.M., Kim I.Y., 2009, Stress rupture predictions of pressure vessels exposed to fully engulfing and local impingement accidental fire heat loads, *Eng. Fail. Anal.* 16, 1141–1152.
- Scarponi G.E., Landucci G., Birk A. M., Cozzani V., 2018, LPG vessels exposed to fire: Scale effects on pressure build-up, *Journal of Loss Prevention in the Process Industries*, 56, 342-358.
- Scarponi G.E., Landucci G., Heymes F., Cozzani V., 2018, Experimental and numerical study of the behavior of LPG tanks exposed to wildland fires, *Process Safety and Environmental Protection*, 114, 251–270.
- Scarponi G.E., Landucci G., Tugnoli A., Cozzani V., Birk A. M., 2017, Performance assessment of thermal protection coatings of hazardous material tankers in the presence of defects, *Process Safety and Environmental Protection*, 105, 393-409.
- Tugnoli A., Gubinelli G., Landucci G., Cozzani V., 2014, Assessment of fragment projection hazard: Probability distributions for the initial direction of fragments, *Journal of Hazardous Materials*, 279, 418-427.